Changes in meteorological parameters during the total solar eclipse of 2 July 2019 in La Serena, Chile

Juan A. Lazzús[*,1,2], Pedro Vega-Jorquera[1], Rene Pacheco[1], Luis Tamblay[1], Miguel Martínez-Ledesma[3,4], Elías M. Ovalle[4,5], Enrique Carrasco[4,6], Manuel Bravo[4,6], Carlos U. Villalobos[4,6], Ignacio Salfate[1], Luis Palma-Chilla[1], and Alberto J. Foppiano[5]

[(1)] Departamento de Física, Universidad de La Serena, Casilla 554, La Serena, Chile

[(2)] Instituto de Investigación Multidisciplinario en Ciencias y Tecnología, Universidad de La Serena, La Serena, Chile

[(3)] Departamento de Astronomía, CePIA, Universidad de Concepción, Concepción, Chile

[(4)] Centro Interuniversitario de Física de la Alta Atmósfera, CInFAA, Chile

[(5)] Departamento de Geofísica, Universidad de Concepción, Concepción, Chile

[(6)] Centro de Instrumentación Científica, Universidad Adventista de Chile, Chillán, Chile

Abstract

The first report on the changes in meteorological parameters during the total solar eclipse of July 2, 2019, in La Serena (Chile), is presented. The event could be observed from morning time on the east of New Zealand, in the South Pacific Ocean, to sunset time in Chile. Several meteorological properties such as global radiation R_g, net radiation R_n, reflected radiation R_r (in Wm^{-2}/min), air temperature (T_A in °C), relative humidity (RH in %), wind speed amplitude (W_S in ms^{-1}), and wind speed direction (W_D in degrees), were recorded with La Serena weather station SER (29.827°S, 71.261°W, 28 masl) at 1-minute time resolution. Importantly, SER was located at 40 km from the axis of the umbra that covered 201 km of width, where it reached 100% darkness at a magnitude of 1.009 during a clear-sky day. Under these auspicious conditions, we observed a rate of changes in the drop of the radiation components of 3.1, 2.4, and 0.5 (Wm^{-2}/min) for R_g, R_n, and R_r, respectively, with a 100% reduction in the components of surface solar radiation (0 Wm^{-2}) during totality. In addition, all components showed a ~34% energy loss during the eclipse in comparison with the day before the event. Also, the rate of changes of −3.3 °C in T_A, +11% in RH, −1.11 ms^{-1} in W_S, and 180° to 340° for W_D in total synchrony with the passing of the moon in front of the sun, reaching respective peaks at ~5 min lag with respect to totality. Thus, our results show a progressive change in all meteorological parameters in total synchrony with the eclipse's phases caused by the passing of the moon in front of the sun.

Keywords: Total solar eclipse; Surface solar radiation; Solar-terrestrial interaction; Micrometeorology; Energy balance

1. Introduction

The scientific community, especially meteorologists, space scientists, and astronomers approach solar eclipses with great interest. Mainly, the impact of solar eclipses has been studied from an astronomical perspective [e.g. Littmann et al., 2008]. But, in space science, their effect on the ionosphere and geomagnetic field has also been analyzed in-depth [e.g. Curto et al., 2006; Bencze et al., 2007, and references therein]. However, the response of the atmosphere to the sudden cut-off of solar radiation only for a few minutes is also of great interest for meteorologists, because such an event can produce disturbance in the atmosphere's dynamics that affect the Earth's environment and biological life [Nymphas et al., 2009]. From the meteorological point of view, these exceptional events have allowed studying the effect of the abrupt disappearance and reappearance of solar radiation on different atmospheric properties [Nymphas et al., 2012].

Over the last decades, several studies have found different meteorological effects as result of solar eclipses. These results show, for example, a decrease in temperature and an increase in relative humidity, as well as changes in wind speed and direction [e.g Anderson et al., 1970; Anderson, 1999; Ahrens et al., 2001; Szalowski, 2002; Gerasopoulos et al., 2008; Hanna, 2000; Founda et al., 2007; Nymphas et al., 2009; Hanna et al., 2016; Ojobo et al., 2017], ozone concentration variations [e.g. Bojkov, 1968; Chakrabarty et al., 1997; Zerefos et al., 2000, 2001; Chudzyński et al., 2001; Winkler et al., 2001; Tzanis et al., 2008], and solar irradiance changes [e.g Kolarž et al., 2005; Ilić et al., 2018]. The studies referred to the magnitude of these changes regarding different eclipse stages, showing that location of the registering station and local environmental conditions are key [e.g. Szalowski, 2002, and references therein]. Besides, it has been accepted that solar eclipses trigger a complex of physical processes in the atmosphere, ionosphere and geomagnetic field [e.g. Akimov et al., 2005]. So, a better study of geophysical effects during an eclipse allows us to improve the understanding of the origin of ionospheric and atmospheric disturbances related to the sun.

During a solar eclipse, the dynamic processes in the atmosphere depend on several factors such as time of day or meteorological and geophysical conditions [see Aplin et al., 2016, and references therein]. In addition, Stankov et al. [2017] examined the importance of geographical location and altitude from which the eclipse is observed to quantify the atmosphere's response to the eclipse's effects. Eclipse meteorology has been recorded mainly at geographical locations in Europe, North America, Asia [see Aplin et al., 2016, and references therein], and Africa [Nymphas et al., 2009, 2012; Ojobo et al., 2017], but for South America only scarce records exist [see Fernández et al., 1993, 1996].

On July 2, 2019, a total solar eclipse occurred in Coquimbo Region, Chile, giving us the opportunity to study its impact on the meteorological variables at this location in the southern hemisphere, at middle latitude (about 30°S, 70°W), and at about the sea level, around 800m away from the coastal edge of the Pacific Ocean. In this contribution, the effects of this total solar eclipse on surface radiation components over the city of La Serena are reported, using data from a weather station which belongs to the Laboratory for Space and Atmospheric Physics and the Department of Physics of the University of La Serena. Note that, several authors have studied the variability of different components of solar radiation during solar eclipses, for example, in recent studies, Blumthaler et al. [2006] employed an extended set of instruments during the total solar eclipse of March 29, 2006, on the Greek island Kastelorizo. Also, Founda et al. [2007] investigated solar radiation variations during the same eclipse in Greece. Later, Hassan and Rahoma [2010] recorded global, direct, and diffuse solar radiation during this event in Tobruq, Libya. Besides, Nymphas et al. [2009, 2012] recorded changes in global radiation, net radiation, and surface energy fluxes during the total solar eclipse of March 29, 2006, in Nigeria. In other studies, Maturilli and Ritter [2016] employed the Baseline Surface Radiation Network station to record the surface radiation during the solar eclipse of March 20, 2015, in Ny-Ålesund (Svalbard), Norway. Schulz et al. [2017] measured the surface energy fluxes during this eclipse in in the same location. Ilić et al. [2018] observed changes in global solar radiation using remote sensing and in situ instruments during the same event in Belgrade, Serbia. In more studies, Peñaloza Murillo and Pasachoff [2018] investigated the impact of cloudiness on global solar radiation during the total solar eclipse on July 22, 2009, in Tianhuangping (Zhejiang), China. More recently, Calamas et al. [2019] measured the temporal variation of the direct radiation, diffuse horizontal, and global horizontal irradiances during the solar eclipse of August 21, 2017, in the United States. More cases can be reviewed in Aplin et al. [2016, and references therein].

On the other hand, this event was not only a unique opportunity for solar radiation observations but also for obtaining rare meteorological records resulting from the sudden disappearance and reappearance of solar energy on several atmospheric environmental parameters as the moon passed in front of the sun. Then, an analysis of the effects of the total solar eclipse on some atmospheric environmental parameters, was made. This analysis was

applied for the most common meteorological properties such as the temperature and relative humidity of the air, and wind speed and direction in the city of La Serena, Chile, in the zone where 100% of darkness was reached during this event.

These four parameters have been widely studied, including during unusual events such as solar eclipses. For example, Ahrens et al. [2001] investigated changes in air temperature, horizontal wind speed, and wind direction by using one meteorological station in the path of totality and another outside the path of totality of the total solar eclipse on August 11, 1999 in Baden-Württemberg, Germany, but with adverse cloudiness conditions. Later, and due to these cloud and precipitation conditions, Vogel et al. [2001] simulated the effects on air temperature and wind using a model with a cloud-free condition for the Upper-Rhine Valley in Germany. Also, Krishnan et al. [2004] observed the impact of this eclipse on temperature, humidity, and wind speed over Ahmedabad, India, with 99.7% obscuration. For the same event, Kolarž et al. [2005] studied changes in air temperature and relative humidity in Belgrade, Serbia, with a partial eclipse at 97.7% darkness. Furthermore, during the total solar eclipse of March 29, 2006, Founda et al. [2007] examined the effects on surface air temperature and wind speed recorded in Kastelorizo, Greece. Pleijel [2008] reported changes in air temperature and relative humidity during this eclipse in Side, Turkey. Besides, Nymphas et al. [2009] investigated changes in the wind speed and air temperature at different heights above the ground in Ibadan, Nigeria. For another eclipse, Chung et al. [2010] observed effects on air temperature, relative humidity and wind speed caused by the partial solar eclipse of July 22, 2009 in Cheongju-Cheongwo, South Korea, with only 81.3% of the sun's maximum. In another event, Hanna et al. [2016] compared data of surface air temperature, wind speed and direction obtained during the solar eclipse on March 20, 2015 between the UK Met Office's automaticweather station and several automatic weather stations in the Faroes Islands and Iceland (with 85%-97% darkness). Also, Ilić et al. [2018] studied the impact of the partial solar eclipse of March 20 (with only 51% darkness) on air temperature, relative humidity, and wind speed over Belgrade in Serbia. Most recently, Ojobo et al. [2017] examined the effects of the annular solar eclipse of September 1, 2016 in Anyigba, Nigeria, on surface air temperature, wind speed, and relative humidity. Similar studies can be reviewed in Aplin et al. [2016, and references therein].

Quantifying the effect of an eclipse on the meteorological parameters is very difficult because of the eclipse's characteristics (type and percentage of obscuration), in addition to the conditions in which it develops as the hour
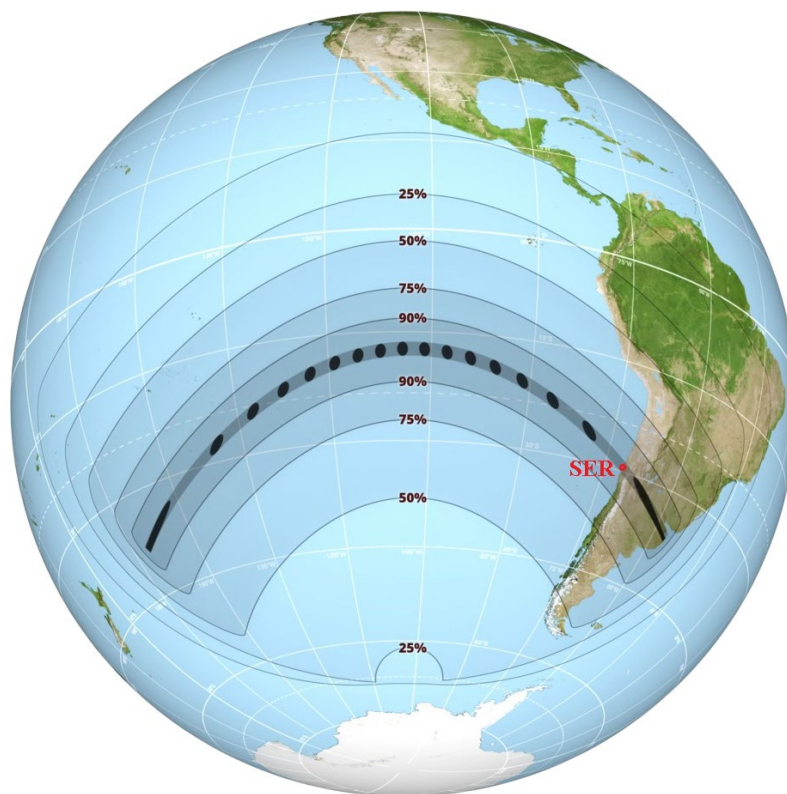
Figure 1. The path of the July 2 total solar eclipse. The map also shows the location of La Serena weather station (SER). Modified from NASA's Scientific Visualization Studio at http://svs.gsfc.nasa.gov/.

of the day, sky conditions, geographical location, among others [see Aplin et al., 2016, and references therein]. In our case, excellent clear-sky conditions and 100% obscuration occurred during the totality on July 2, 2019, in La Serena. Additionally, the unusual circumstances in which it occurred (at the noon-sunset phase and just before sunset time) added unique characteristics for studying their effects on the meteorological parameters of this location. Hence, changes in the global solar radiation, net radiation, and reflected radiation, air temperature, relative humidity, wind speed, and wind direction were recorded with in situ instruments by using La Serena weather station (SER). The privileged location of the SER station for investigating this event, only a few kilometers from the umbra's center (29.827°S and 71.261°W), at about sea level and near the coastal edge of the Pacific Ocean, highlight the importance of this study (Figure 1). According to our knowledge, this is the first report of the effects of this eclipse on the meteorological parameters in any of the areas in its path, and the first report of this type for Chile.

2. Total solar eclipse of July 2, 2019

Only three solar eclipses had been registered in Chile's Coquimbo Region: (1) on June 9, 1592, with totality duration of 3 minutes and 54 seconds; (2) on March, 15, 1839, with totality lasting 2 minutes and 36 seconds (but, lack of technology prohibited obtaining sophisticated records, aside from photographic data [Obrecht, 1893]); and (3) on April 16, 1893, including the territory of Chile's Atacama Region [Association of Universities for Research in Astronomy, 2019].

The total solar eclipse of July 2, 2019 was seen along the Pacific Ocean, in Chile, and at sunset in Argentina (see Figure 1). The eclipse shadow was a narrow band and about 200 km wide. The path of the moon's umbra traveled 11,252 km from west to east, beginning in the morning in the South Pacific, east of New Zealand, and moving northeast. Then it took a southeastern direction and passed by Chile until sunset. It could be partially observed in many parts of southern South America.

In the city of La Serena (Coquimbo Region), the umbra reached 100% darkness and had a width of 201 km. The axis of the totality strip was at 41 km to the north of this city. This city hosts La Serena weather station, or SER (see Figure 1). Specific solar eclipse data for La Serena include: an eclipse magnitude of 1.009, the eclipse starts at 15:22:34.5 hr LT, eclipse end 17:46:36.0 hr LT, and maximum phase at 16:39:21.4 hr LT at an altitude of 13.5° above the horizon, and totality lasting for 2 minutes and 12 seconds. As complementary information, this eclipse belongs to the Saros 127 series (58 of 82) Catalog No. (SE5000) 9551 [https://eclipse.gsfc.nasa.gov/SEsaros/SEsaros127.html].

3. Measurement site and instrumentation

Meteorological data were recorded by SER in the facilities of the University of La Serena's Laboratory for Space and Atmospheric Physics belonging to the Department of Physics. This center in Villa Juan Soldado district is on the city's outskirts and far from greater urban settlements. Its coordinates are 29.827°S and 71.261°W, positioned on an extensive plateau at 28 masl, and at 800 m from the coastal of the Pacific Ocean in plain territory (see Figure 1).

The SER station has several instruments that record various meteorological parameters. The calibration of instruments and quality of meteorological parameters from these instruments are maintained as per World Meteorological Organization (WMO) and the Chilean Meteorological Service standards. All sensors were installed 1.5 m above ground (which at this site is characterized by dry sandy clay soil with sparse vegetation) and calibrated at 1 min time resolution. Table 1 shows a technical description of the instruments used.

On July 2, clear skies prevailed during the entire path of the eclipse in Chile, including the location of the SER station (see Figure 2). Clear sky conditions have greater importance for assessing the surface solar radiation during the eclipse [Peñaloza Murillo and Pasachoff, 2018]. Another important factor is the effective sun hours [Reda, 2015]. For this date, Chile was in winter season with sort days of ~10 hr. Specifically, on July 2, the sunrise was recorded ~07:50 hr LT, while the sunset was ~17:50 hr LT. In addition, the eclipse occurred during the noon-sunset phase of this day between 15:22:34 and 17:46:36 hr LT. Additionally, to contrast the average weather conditions for July 2 and July 1, Table 2 shows this comparison for the time windows before, just during, and after the eclipse.

Moreover, the climate of the city of La Serena is defined as coastal steppe with cloudiness [Avaria et al., 2004], or cold semi-arid climate [Geiger, 1954, 1961], and it is located in a transition zone between the hyper-arid Atacama Desert (northern Chile) and central Chile's Mediterranean climate [Veit, 1993]. In addition, it is strongly affected

Sensor	Device and model	Measuring range	Spectral response/ Accuracy	Operating range	Sensitivity
Global radiation	GS1-05 Pyranometer Dome solarimeter	0 to 2 kWm^{-2}	305 to 2800 nm	−40 to +80 °C	10-35 mV/kWm^{-2}
Net radiation	NR2-07 Dome net radiometer	0 to 1 kWm^{-2}	0.25 to 60 mm	−40 to +60 °C	100 mV/kWm^{-2}
Albedometer	GS1-05 and GS2-05 Dome solarimeters mounted back to back	0 to 2 kWm^{-2}	305 to 2800 nm	−40 to +80 °C	10-35 mV/kWm^{-2}
Air temperature	AT1 Air temperature sensor, 2k thermistor	−10 to +105°C	±0.1 °C	−30 to +70°C	10 mV per °C
Relative humidity	RH1 Cylindrical louvered solar radiation shielded housing	0 to 100%	±2% at 23°C	−30 to +70°C	10 mV per %RH 0-1 V for 0-100%
Wind speed	AN1 Anemometer, mercury-wetted reed switch type. 3-cup rotor	0.2 to 75 ms^{-1} (170 mph)	1% ±0.1 ms^{-1} (0-55 ms^{-1}) 2% (>55 ms^{-1})	−30 to +70°C	0.8 Hz per ms^{-1}
Wind direction	WD1 Wind vane Sturdy and highly responsive, based on micro-torque potentiometer	0 to 358 degrees	0.3° (resolution) ±2° in winds >5 ms^{-1} starting threshold 0.6 ms^{-1}, 45° to flow	−50 to +70°C	2.8 Ω per degree

**Table 1.** Technical details of the instruments used by SER station.

	July 2			July 1		
	TW*	TW**	TW***	TW*	TW**	TW***
Temperature	12 °C	14 °C	12 °C	12 °C	13 °C	11 °C
Relative humidity	53%	44%	52%	55%	47%	53%
Wind speed	1.3 ms^{-1}	1.2 ms^{-1}	1.4 ms^{-1}	1.3 ms^{-1}	1.6 ms^{-1}	0.3 ms^{-1}
Wind direction	northeast	southwest	northeast	northeast	northeast	northeast

TW*: the time window from sunrise until just before the eclipse.
TW**: the time window during the eclipse.
TW***: the time window from just after the eclipse until the sunrise.

Table 2. Comparison of the average weather conditions for July 2 and July 1.
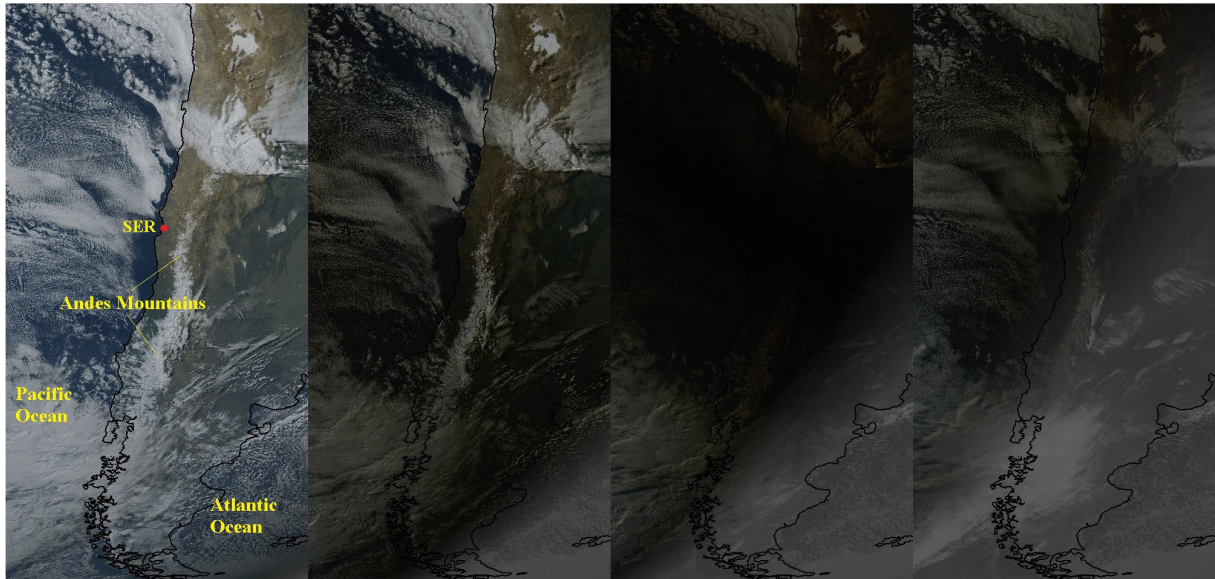
Figure 2. Clear sky conditions observed for the zones in the path of the eclipse on July 2, 2019. Image generated from the GOES-East (GOES-16) and GOES-West (GOES-17) satellites True Color RGB imagery (https://www.goes.noaa.gov/). As shown, clear sky conditions prevailed during the day and for all phases of the eclipse (images from left to right). This Figure shows a general picture of the passage of the eclipse's shadow through a wide window of clear sky.

by interacting atmospheric, oceanic, and orographic factors such as El Niño/LaNiña-Southern Oscillation (ENSO), the South-east Pacific Subtropical Anticyclone (SPSA), the Humboldt Current System (HCS), the Madden-Julian Oscillation (MJO), the complex topography of Chilean east-west transverse Elqui valley, and the Andes Mountains [Kalthoff et al., 2002; Bischoff-Gauß et al., 2008; Fiebig-Wittmaack et al., 2012; Juliá et al., 2012; Ancapichún and Garcés-Vargas, 2015]. Besides, this zone includes complex weather characteristics that extend from the cold South Pacific Ocean in the west to the Andes in the east, with an average height of about 5,000 masl [Kalthoff et al., 2002]. Thus, to discard any local weather effects that may have affected these meteorological parameters during the eclipse, we analyzed each sensor recording separately.

4. Data analysis

4.1 Solar radiation

Figure 3 shows a comparison between the data recorded by SER station for different components of the surface solar radiation during the day before (July 1) and the day of the eclipse (July 2). For better analysis, we considered only the time window of the eclipse (180 minutes) on both days. In addition, all panels have highlighted the moments of the eclipse with vertical red lines for the start and end, and with a vertical black line for its maximum. Specific solar radiation components are listed as: (*a*) global radiation R_g, (*b*) net radiation R_n, and (*c*) reflected radiation R_r. Contrasting the curves for both days, all graphics for July 2 display a progressive decrease of all components of surface solar radiation from the start to the maximum phase at 16:39:21 hr LT with minima values of about 0 Wm^{-2}. According to these observations, there were remarkable variations for all components of the surface solar radiation during the eclipse on July 2.

Figure 3*a* shows the comparison between the measurements of solar global radiation recorded during July 1 and 2 at the time of the eclipse. On July 2, when the eclipse started at 15:22:34 hr LT, R_g recorded 236.029 (Wm^{-2}), progressively decrease until the maximum eclipse to 0 (Wm^{-2}) at 16:39:21 hr LT. Then, it slighty but steadily increased until coinciding with the usual R_g behavior during sunset, almost coinciding with the end of the eclipse at 17:46:36 hr LT. R_g then show an equal percentage of reduction in line with the percentage the moon hid the sun during the first phase until totality at 100% darkness with 100% reduction of R_g. Note that the changes recorded by
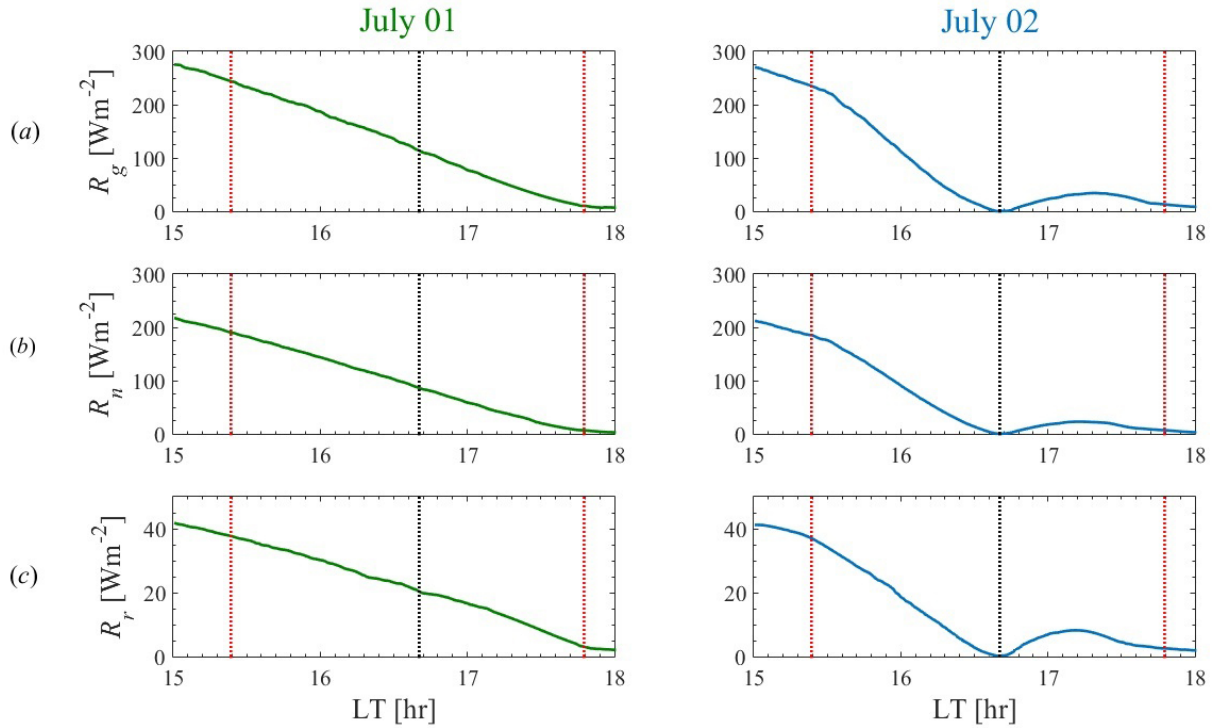
Figure 3. Comparison between the data recorded for different components of surface solar radiation during the day before and the day of the eclipse (July 1 and 2, respectively). Data were measured at La Serena weather station at 1 min resolution. From top to bottom panels: (a) global radiation, (b) net radiation, and (c) reflected radiation. Here, vertical red lines denote the start and end of the eclipse, and the vertical black line represents the maximum eclipse at a time window of 180 min centered on its maximum phase.

SER are comparable to the results obtained by Founda et al. [2007] during the total solar eclipse of March 29, 2006, in Greece, and by Nymphas et al. [2012] during the same event in Nigeria, and with others studies (see Section 1).

To quantify the lost energy for R_g during the eclipse, we use the solar irradiation (energy) as the area under the R_g curve. Figure 4a illustrates the lost energy during the eclipse on July 2 in comparison with the accumulated energy on July 1 at the same time window. As shown, on July 2 there was a 33.9% less energy than July 1 due to the eclipse.

Also, to investigate the changes the eclipse caused on net radiation, we compared data recorded on the eclipse day (July 2) and data measured the day before (see Figure 3b). On eclipse day, R_n recorded 185.5 (Wm^{-2}) just at the start of the event and values dropped progressively until totality to 0 (Wm^{-2}) at 16:39:21 hr LT to later increase progressively until falling to usual R_n values at sunset by the end of the eclipse at 17:46:36. This 100% reduction of R_n at maximum eclipse is comparable to the findings by Ahrens et al. [2001] during the total solar eclipse of August 11, 1999, in Germany, and by Maturilli and Ritter [2016] during the total solar eclipse of March 20, 2015, in Norway, among other studies (see Section 1). Here, the percentage of the drop of R_n was also proportional to the obscuration percentage.

To determine the effect of the eclipse on the lost energy for R_n during its phases, we calculated the irradiation values of R_n for July 1 and 2 (see Figure 4b). As a direct effect of the eclipse, on July 2 there was a 33.0% less energy than July 1 during the same time window.

With respect to reflected radiation, Figure 3c shows the comparison between the data recorded in the same time window for the eclipse on July 1 and July 2. On July 2, at the start the eclipse, R_r recorded 37.190 (Wm^{-2}), which decreased to 0 (Wm^{-2}) at 16:39:21 hr LT in the maximum phase of eclipse. Next, R_r slightly but steadily increased until coinciding with normal sunset values by the end of the eclipse. In this case, the 100% darkness at the totality generated a 96% reduction of R_r.

Figure 4c shows the lost energy during the eclipse on July 2 in comparison with the accumulated irradiation on July 1 at the same time window. As can be observed, on July 2 there was a 34.4% less energy for R_r than July 1 as a direct consequence of the eclipse.
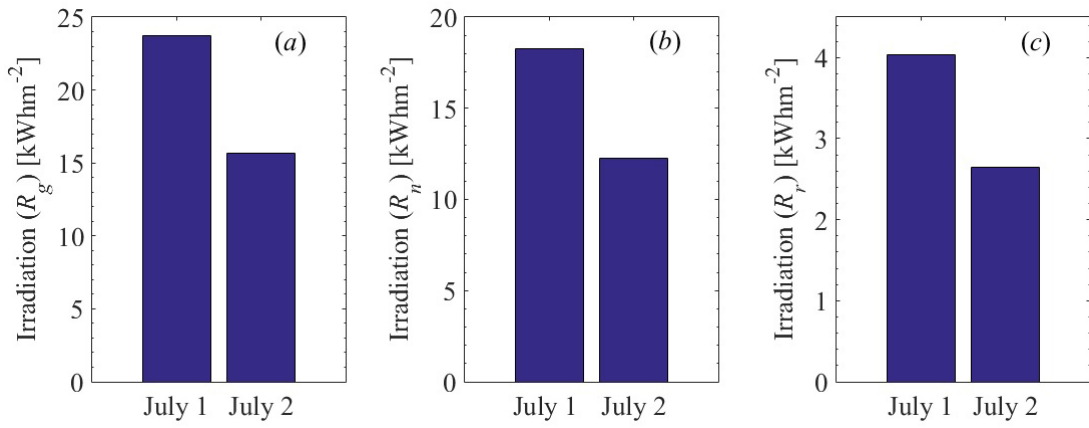
Figure 4. Comparison between the solar irradiation (energy) accumulated on July 1 and July 2 at the same time window that eclipse. From left to right panels: (a) global radiation, (b) net radiation, and (c) reflected radiation.

4.2 Air temperature

On the other hand, Figure 5 shows a comparison between the data recorded by SER weather station for different meteorological parameters during the day before the eclipse (July 1) and the day of the eclipse (July 2) with 1 min resolution and during a local time window from noon to sunset. Here, all panels have highlighted the moments of the eclipse with vertical red lines for the start and end of the eclipse, and with a vertical black line for its maximum. Specific parameters are listed as: (a) air temperature T_A in °C, (b) relative humidity RH in %, (c) wind
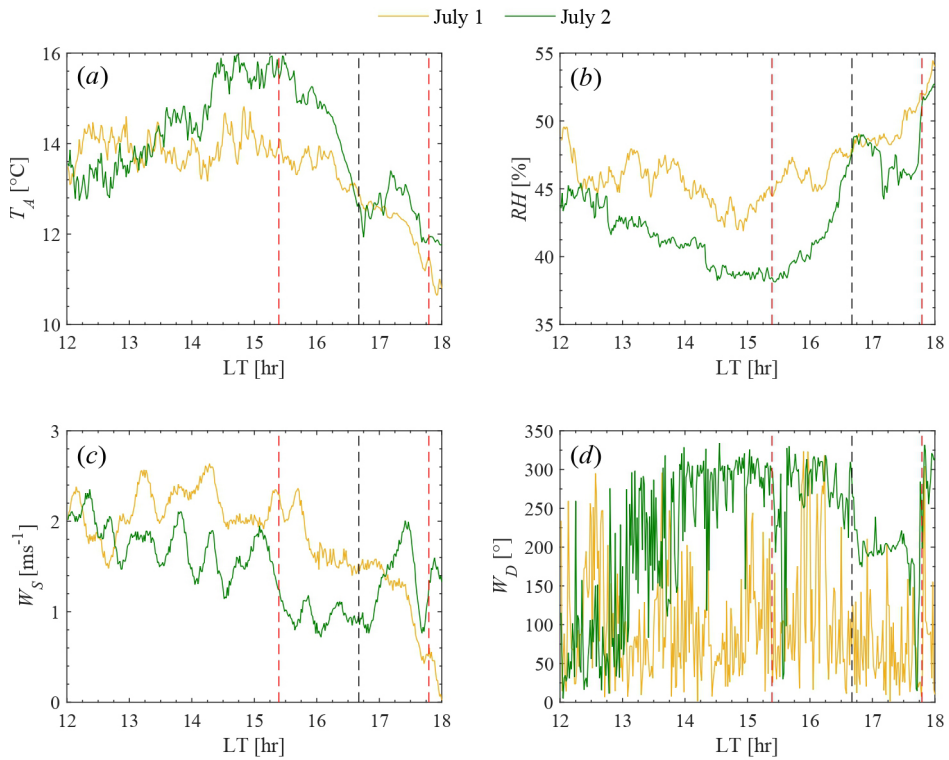
Figure 5. Comparison between the data recorded for different meteorological parameters during the day before and the day of the eclipse (July 1 and 2, respectively). Data were measured by SER station at 1 min resolution. (a) Air temperature, (b) relative humidity, (c) wind speed, and (d) wind direction. In all panels, vertical red lines denote the start and end of the eclipse, respectively, and the vertical black line is the maximum eclipse.

speed amplitude W_S in ms^{-1}, and (d) wind speed direction W_D in degrees. As shown, all graphics exhibit remarkable variations during the eclipse on July 2 in contrast to the day before.

Figure 5a shows a gradual decrease of air temperature during the first phase of the total eclipse, of −3.3 °C with a rate of change of +0.081 (°C/min), reaching the minimum ~5 min after totality. Then occurs a slight increase of +1.5 °C at a rate of +0.122 (°C/min) until it coincides with the usual behavior of T_A during sunset almost coinciding with the end of the eclipse at 17:46:36 hr LT. In contrast, on July 1, T_A exhibits its usual behavior from noon to sunset with a mean of ~13 °C. As observed, the rapid obscuration due to the eclipse does not allow cooling at the same rate as during sunset on a non-eclipse day. Note that the rate of T_A change recorded by SER during the eclipse does not compare to the rates recorded during the same time window for any day of the winter season in La Serena. For instance, in La Serena, the winter season lasts ~3 months, from mid-June to September. The coldest days of the year occur in early July, with an average low of 10 to 12 °C and a high of ~16 °C, with a rate of change of +0.023 (°C/min). Also, T_A variation during a year covers from ~−3 to ~30 °C [Lazzús and Salfate, 2017]. However, none of these temperature changes occur at rates as remarkable as the temperature drops recorded during the eclipse. Besides, the stronger phenomena that affect the climate of La Serena such as ENSO, SPSA, HCS, and MJO only show rates of change for a longer time, e.g. +1/−1 (°C/year) for the annual mean temperature during the ENSO events [Schulz et al., 2011]; +0.14 (°C/decade) in annual mean temperature for the period 1960-1992 [Rosenbluth et al., 1997] and −0.20 (°C/decade) for annual mean temperature for the period 1979-2006 [Falvey and Garreaud, 2009] also during ENSO cycles; or a decreasing rate of −0.33 °C/decade (−0.12 °C/decade) in maximum (minimum) temperature for the period 1977-2008 caused by ENSO-IPO (Interdecadal Pacific Oscillation, [see Mantua et al., 1997; Power et al., 1999]) interaction [Schulz et al., 2011]. Thus, having discarded any other external factors affecting air temperature on July 2, we report a T_A drop in total agreement with the eclipse phases.

Furthermore, our T_A data show the same behavior described by Anderson [1999], where the cooling starts with a lag when the sun started to be covered, later reaching its minimum value with another lag of less than half an hour after totality. This lag is caused by the thermal inertia of the surface layer due to processes controlled by the mass, energy and momentum transport [Ahrens et al., 2001; Aplin and Harrison, 2003; Gerasopoulos et al., 2008; Aplin et al., 2016], in addition to unique characteristics of each event such as the location, height, hours of day, the local climate, clear-sky conditions, site, surrounding vegetation, among others [Ahrens et al., 2001; Aplin et al., 2016]. Besides, our maximum T_A change of −3.3 °C with a rate of +0.081 (°C/min), is consistent with the maximum changes reported in the literature [Vogel et al., 2001; Akimov and Chernogor, 2010; Aplin et al., 2016].

Particularly, our results are comparable to those reported by Akimov and Chernogor [2010] during the partial solar eclipse of August 1, 2008, in Kharkov (Ukraine), with an T_A drop of −2 °C at 5 min lag of maximum eclipse, but only at 42% obscuration, and for a site with humid continental climate [Geiger, 1954, 1961]. Also, for the eclipse of August 11, 1999, in Plittersdorf (Germany), Ahrens et al. [2001] reported an T_A drop of ~−2 °C with 5 min lag from totality at 100% darkness, but with unfavorable cloudiness conditions, and at a site with temperate oceanic climate [Geiger, 1954, 1961]. However, at similar T_A changes, remarkable differences between these events emerge as the total eclipse in La Serena occurred with 100% darkness, at clear-sky conditions, and in cold semi-arid (steppe) climate [Geiger, 1954, 1961]. In addition, the site conditions in La Serena during the total eclipse are akin to those reported by Krishnan et al. [2004] for the eclipse of August 11, 1999, in Ahmedabad (India), with 99.7% obscuration, but for a cold semi-arid climate [Geiger, 1954, 1961]. However, these authors report a temperature decrease of only ~−0.5 °C. Note that the pattern and the precise T_A declines vary significantly from one event to another [Nymphas et al., 2009], however, the general temperature behavior recorded during this eclipse is in line with that reported by several authors analyzing other eclipses. For example, for the eclipse of March 29, 2006, in Greece, Gerasopoulos et al. [2008] reported T_A drop of 3.9 °C, while Economou et al. [2008] reported a drop of 2.2 °C, also Founda et al. [2007] observed drops between 1.6 and 3.9 °C with 12-14 min lags after maximum eclipse, with rates between 0.030 and 0.055 (°C/min). For the same event, Nymphas et al. [2009] recorded a drop of 1.6, 1.0, and 0.8 °C at heights of 1, 6, and 12 m, respectively, during this eclipse in Nigeria. In other studies, Ilić et al. [2018] observed an T_A decrease of −2.6 °C at the rate of 0.043 (°C/min), reaching minimum about 15 min lag during the partial solar eclipse of March 20, 2015, in Belgrade (Serbia) with 51% darkness. Anderson [1999] compiled T_A data for a set of selected total eclipses reported in the literature and showed decrease from 2.0 to 3.6 °C, with minimal values reached from 7 to 17 min lags after totality. More examples with similar drops, rates, and lags can be reviewed in Aplin et al. [2016, and references therein]. But the values reported in these studies can also differ from those reported in a more recent study, such as Calamas et al. [2019], who observed an T_A drop of 8.49 °C with 47 min lag after totality, during the eclipse of August 21, 2017, in the United States.

4.3 Relative humidity

Figure 5b shows a fast and gradual increase of +11% of relative humidity between the early and maximum eclipse, with a rate of change of 0.26 (%/min), peaking at a 5 min lag with respect to totality. After the maximum, RH decreases −5% at a rate of 0.33 (%/min), then recovers its usual behavior during sunset coinciding with the end of the eclipse. On the other hand, on July 1, RH data describe the characteristic behavior during the daytime, with a gradual decrease from sunrise to noon (typically between 14 to 15 hr LT) followed by a gradual increase until the sunset and nighttime. Contrasting both curves, we observed an unusual behavior of RH on July 2 during the time window of the eclipse. We also observed an anticorrelation with T_A data relating directly +10% RH increase with the −3.3 °C T_A drop as a consequence of the cooling during the eclipse (Figure 5a).

Relative humidity has an inverse relationship with air temperature, thus, during an eclipse, RH changes are typically dominated by T_A changes [Aplin et al., 2016]. In the literature, eclipse effects on RH have been reported to a much lesser extent than effects on T_A, however, some reports can be compared with our results. For example, Chung et al. [2010] observed a RH increase of +3.4% during the eclipse of July 22, 2009 in Cheongju-Cheongwo (South Korea), but with only 81.3% darkness. Also, Ojobo et al. [2017] reported an increment of +6% during the annular solar eclipse of September 1, 2016, in Anyigba (Nigeria). Namboodiri et al. [2011] reported a variation of +19% during the annular solar eclipse of January 15, 2010 in Thumba (India), but with 28 min lag after totality. All these reports present RH increments in agreement with our result although obscuration and time-lags differ greatly with La Serena data obtained with 100% darkness and 5 min lag after the maximum eclipse. However, these reports show the same reverse observations between RH and T_A as in La Serena. In contrast, some reports contradict this relationship, e.g. Nishanth et al. [2011] observed a RH drop of −6.4% also associated with an T_A drop of −2 °C during the eclipse of January 15, 2010, in Kannur (India). In addition, Ilić et al. [2018] reported that RH remained almost constant during the eclipse of March 20, 2018, in Belgrade (Serbia). Also, Krishnan et al. [2004] reported that RH did not show any appreciable variation during the eclipse of August 11, 1999 in Ahmedabad (India). This rare behavior reported for RH can be attributed to less ideal weather conditions to investigate the effect of those solar eclipses on air humidity [Ahrens et al., 2001].

In other aspect, the average humidity is 70% in La Serena and includes a high seasonal gradient where average relative humidity reaches 30% and 60% at 14:00 and 15:00 hr LT during summer and winter respectively, while average relative humidity can increase up to 90% during nighttime between 21:00 and 00:00 hr LT for any season [see, http://www.ceazamet.cl/]. Other remarkable RH variations can be observed in La Serena during the last ENSO events, e.g. changes of ∼30 (%/cycle) between La Niña 2012 and El Niño 2015 events [National Oceanic and Atmospheric Administration, 2017]. Because seasonal and ENSO variations show the rate of change at longer time, the significant changes recorded for RH during the eclipse of July 2 can be attributed to the impact of the solar eclipse on the surface energy balance over La Serena.

4.4 Wind

As observed in Figure 5c, the effect of the total solar eclipse on wind speed shows an erratic but progressive decrease of W_S during the initial phase of the eclipse with a rate of change of 0.037 (ms^{-1}/min) from 1.82 ms^{-1} until 0.71 ms^{-1} (−1.11 ms^{-1}) with two short increasing peaks but clear tendency to drop before totality, followed by an erratic recovery behavior, dropping again at ∼5 min lag with respect to totality. Until this hour, the W_S for July 1 had a rate of change of −0.06 (ms^{-1}/min) showing an erratic behavior (but also characteristic for this zone [Kalthoff et al., 2002]) during the daytime with a predominant tendency to calm until the nighttime regime starts. But, on July 2, W_S increased after the maximum eclipse at a rate of +0.058 (ms^{-1}/min) with an increment of +1.24 ms^{-1}, then recovered its usual behavior near the end of the eclipse at a rate of ∼−0.06 (ms^{-1}/min). Note that this observed behavior on W_S is compatible with "Clayton's phenomenon" [Clayton, 1901] where the effect of the lunar shadow generates atmospheric circulation changes, yielding reduced wind speed with a profound change of wind direction [Harrison and Gray, 2017]. Effectively, Figure 5d shows remarkable differences between the behavior of W_D on July 1 and 2, mainly during the time windowof the eclipse. Clayton' phenomenon has been attributed to several atmospheric processes. For example, early observers describe bursts of a cold front in the penumbra before or after the eclipse [Klein and Robinson, 1952; Anderson and Keefer, 1975]. Antonia et al. [1979] found that the surface layer turbulence just responds to stability changes caused by the abrupt change in surface heat flux. Fernández et al. [1993] suggested

that due to the decrease in temperature during the total solar eclipse on July 11, 1991, in Costa Rica, the thermal gradient decreased on the mesoscale and synoptic-scale and, consequently, the wind speed too. Later, during another eclipse, Fernández et al. [1996] found the decrease in wind speed was due to the cooling and gradual stabilization of the atmosphere, similar to what is observed at sunset. Also, this phenomenon has been attributed to gravity waves associated with a strong cooling in the upper stratosphere and/or an enhanced wind chill effect caused by the eclipse [Anderson, 1999; Winkler et al., 2001]. In addition, several modeling studies have predicted similar effects to those of Clayton's phenomenon [Prenosil, 2000; Aplin and Harrison, 2003; Gray and Harrison, 2012].

On the other hand, at La Serena, wind data show that wind speed reaches a maximum amplitude of $\sim$9 ms^{-1} in summer and $\sim$4 ms^{-1} in winter [Salfate et al., 2018]. Also, Lazzús and Salfate [2017] estimated mean wind speed of $\sim$3 (ms^{-1}/day), while Salfate et al. [Salfate et al., 2018] show a rate of change of $\sim$3 (ms^{-1}/year) of annual mean wind speed. Additionally, the stronger phenomena that affect its climate, such as ENSO, SPSA, HCS, MJO, and Coriolis Force create the conditions for the prevailing northeasterly annual mean wind direction [Kalthoff et al., 2002; Juliá et al., 2012; Ancapichún and Garcés-Vargas, 2015]. Besides, it contribute to westerly wind prevailing in summer, while the contributions to westerly and easterly winds are nearly the same during winter [Kalthoff et al., 2002]. However, all these changes regarding wind occur in the long term, foregoing comparability with the narrow time window in which this eclipse occurred. Thus, having discarded any previous phenomena as causes of the wind speed drop during the eclipse time-lapse, we believe that a Clayton-type phenomenon occurred due to the effect the eclipse had on atmospheric circulation. While these changes in wind speed are already being discussed in the literature, those must always be accompanied by changes in the wind direction and other atmospheric properties. Effectively, data recorded by SER station show a drop in wind speed and remarkable changes in wind direction during the solar eclipse phases (Figs. 5c and 5d). To clarify these changes in the W_D, we used wind rose diagrams. Figure 6 presents a comparison of wind direction data recorded by SER station on June 30, July 1 and July 2. Here, the left column shows the wind regime measured during the two hours before the start of the eclipse, and the right column shows wind regime measured during the time window of the eclipse. Note that the records obtained during June 30 and July 1 follow the northeasterly regime that is the prevailing annual mean direction over this zone [Kalthoff et al., 2002; Juliá et al., 2012; Ancapichún andGarcés-Vargas, 2015], while on July 2 the onset of southwesterly wind during the eclipse time-lapse is observed with a shift in W_D from 180° to 340° (see, Figure 6f).

In addition, wind data recorded by SER station is in agreement with other observations reported in the literature. For example, Ahrens et al. [2001] presented a W_S drop of $\sim$−1 ms^{-1} during the solar eclipse of August 11, 1999 in Baden-Württemberg, Germany. During the same event, Aplin and Harrison [2003] reported a W_S drop of −2 ms^{-1} with a shift in W_D about 130° to 140°, in Camborne, U.K. Also, Nymphas et al. [2012] reported drops of $\sim$−1 ms^{-1} during the solar eclipse of March 29, 2006, in Ibadan, Nigeria. Schulz et al. [2017] observed W_S drops of $\sim$−1.5 ms^{-1} and W_D changes from 180° to 225° during the total solar eclipse in Svalbard.

5. Discussion

Our analyses demonstrated a progressive decrease in all components of surface solar radiation in synchrony with the passing of the moon in front of the sun. During the time window of the eclipse, all components showed a $\sim$34% energy loss in comparison with the day before the event. The rate of changes during the drop of surface radiation was estimated at 3.1, 2.4, and 0.5 (Wm^{-2}/min) for R_g, R_n, and R_r, respectively (see Figure 4). These reduction in the components of surface solar radiation and their analyzed effects on the energy balance/flux agree with reports based on other eclipses [e.g. Ahrens et al., 2001; Founda et al., 2007; Nymphas et al., 2012; Maturilli and Ritter, 2016]. However, given the special conditions under which the latest eclipse unfolded, and under which it was observed from the SER station, these conditions could also be strongly related to the drop of solar radiation during the event. Note that Stankov et al. [2017] explained the effects the eclipse geometry (with respect to its geographic location) has on the atmosphere by relating them to the different altitudes at which the lunar shadow crosses it. For the SER station location, the eclipse started at an altitude of 25.5° above the horizon (at 15:22:34 hr LT) and ended at an altitude of 1.1° above the horizon (at 17:46:36 hr LT) including a few minutes of sunset. According to Stankov et al. [2017] at these altitudes, all the effect of the total solar eclipse of July 2 in La Serena were directly and entirely on the stratosphere and troposphere layers.

In addition, the eclipse altitude alters the atmospheric processes in all strata and affects observations at ground level [Gerasopoulos et al., 2008], wherein several cases it is impossible to distinguish the particular contribution
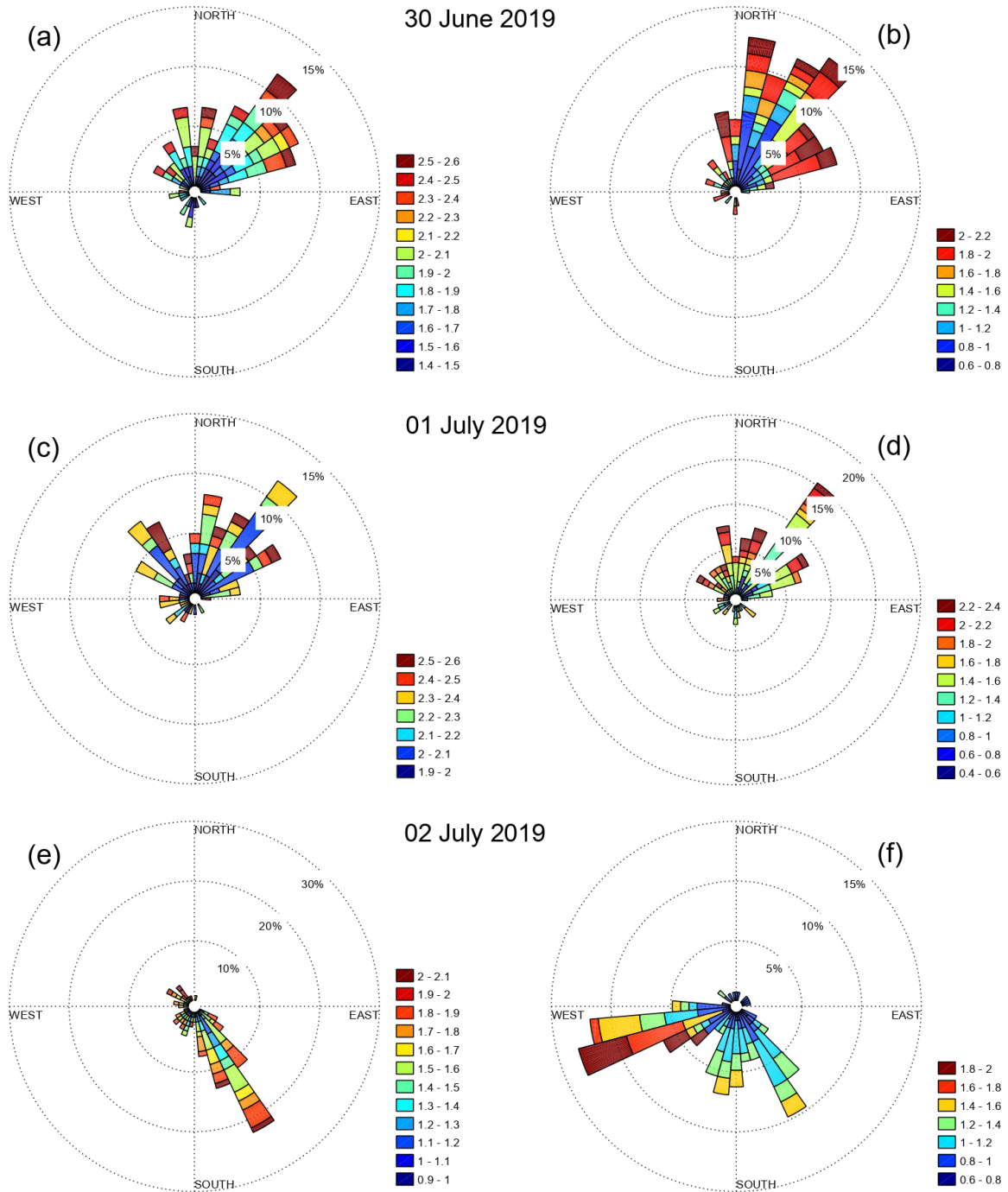
Figure 6. Comparison of wind direction data recorded by SER station on June 30, July 1 and July 2 (panels top to bottom, respectively). In all cases, the left column shows the wind regime measured during the two hours before the start of the eclipse, and the right column shows wind regime measured during the time window of the eclipse.

of each atmospheric process separately [see Aplin et al., 2016, and references therein]. To investigate these effects on the data from July 2, Figure 7 presents the eclipse's altitude and the visible fraction of the sun during its phases in superposition with the meteorological properties recorded by SER. This Figure also shows an overview of the changes in these properties during the total eclipse.

At SER coordinates (29.827°S, 71.261°W, 28 masl) the eclipse starting at 25.5° and decreasing until 1.1°. Note that this low altitude is due to the southern hemisphere's winter season, and on July 2 sunset occurred at ~17:56 hr LT at this location. Also, according to Stankov et al. [2017] at these altitudes, the umbra directly affected the lower atmosphere. Effectively, our records show a direct effect on the meteorological parameters with remarkable changes such as −3.3 °C in T_A, +11% in RH, −1.11 ms^{-1} in W_S, and 180° to 340° in W_D during the eclipse (reaching
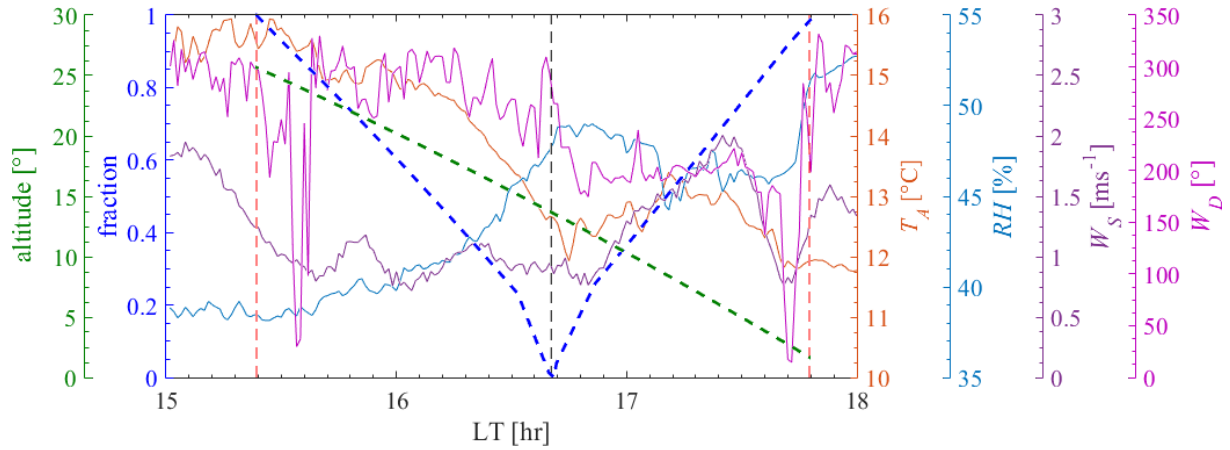
Figure 7. Altitude and the visible fraction of the sun during the eclipse phases in superposition with the meteorological properties recorded by SER station on July 2. Here, vertical red lines denote the start and end of the eclipse, respectively, and the vertical black line is the maximum eclipse.

their respective peaks at ∼5 min lag with respect to totality), and in total synchrony with the passing of the moon in front of the sun as is evidenced in the curve of the visible fraction of the sun. As mentioned, this geographical zone is strongly affected by several atmospheric, oceanic, and orographic factors [Kalthoff et al., 2002; Bischoff-Gauß et al., 2008; Fiebig-Wittmaack et al., 2012; Juliá et al., 2012; Ancapichún and Garcés-Vargas, 2015], but these were practically suppressed by the direct effect of the total eclipse, then recover their normal regimes at the end of this event.

In another aspect, to our best knowledge, this is the first report on the changes of meteorological parameters during the total solar eclipse of July 2, 2019. Here, we present information and measurements which are of invaluable for further scientific investigations. Thus, the scientific community gets a unique and complete set of basic high-quality meteorological data collected during a total solar eclipse under cloudless conditions, recorded at an in-situ station.

6. Conclusions

During the total solar eclipse on July 2, 2019, we analyzed the changes in the meteorological properties in La Serena, Chile, where the umbra reached 100% darkness, and clear-skies condition; then global radiation R_g, net radiation R_n, reflected radiation R_r, air temperature T_A, relative humidity RH, wind speed amplitude W_S, and wind speed direction were recorded at 1 min time resolution by La Serena weather station (29.827°S, 71.261°W, at 28 masl) during all eclipse phases, starting at 15:22:34 hr LT, ending at 17:46:36 hr LT, with maximum phase occurring at 16:39:21 hr LT.

Based on the data analysis and discussions in this study, these main conclusions obtain:

(i) Our results show a progressive decrease in all components of the surface solar radiation (R_g, R_n, and R_r) in total synchrony with the eclipse phases, with a 100% reduction in the components of surface solar radiation (0 Wm^{-2}) during totality. The rate of changes for the fall in radiation components was estimated as 3.1, 2.4, and 0.5 [Wm^{-2}/min] for R_g, R_n, and R_r, respectively. Besides, all components had a ∼34% energy loss during the eclipse in comparison with the day before the event and within the same time window.

(ii) Given the special conditions under which the eclipse developed and under which it was observed from the SER station, our records show an direct effect on the meteorological parameters with remarkable changes such as −3.3 °C in T_A, +11% in RH, −1.11 ms^{-1} in W_S, and 180° to 340° in W_D recorded in the time window of the eclipse (reaching their respective peaks at ∼5 min lag with respect to totality), and in synchrony with the passing of the moon in front of the sun. These results are comparable to those reported by several authors for similar events around the world.

(iii) This eclipse was monitored in a geographical zone that is strongly affected by several atmospheric, oceanic, and orographic factors (see Section 4), but these factors were practically suppressed by the direct effect of the

total eclipse. Besides, all the changes in the meteorological parameters caused by these factors occur over long periods that cannot be compared with the short time window in which this eclipse occurred. Thus, we discarded any of these phenomena as the cause of the remarkable changes in the R_g, R_n, R_r, T_A, RH, W_S, and W_D during the eclipse time-lapse.

(iv) SER station recorded a unique and complete set of high-quality meteorological data of high quality during this total solar eclipse at 1 min time resolution. The University of La Serena's Laboratory for Space and Atmospheric Physics (LAFESAT) implemented quality infrastructure that guaranteed SER's correct operation. The resulting data set is invaluable for further scientific investigations.

References

Ahrens, D., M.G. Iziomon, L. Jaeger, A. Matzarakis and H. Mayer (2001). Impacts of the solar eclipse of 11 August, 1999 on routinely recorded 200 meteorological and air quality data in South-West Germany, Meteorol. Z., 10, 215-223.

Akimov, A.L. and L.F. Chernogor (2010). Effects of the solar eclipse of August 1, 2008, on the earth's lower atmosphere, Kinemat. Phys. Celest. Bodies, 26, 135-145.

Akimov, L.A., E.I. Grigorenko, V.I. Taran and L.F. Chernogor (2005). Features of the Atmospheric-Ionospheric Effects of the Solar Eclipse of May 31, 2003: Results of Optic and Radar Observations in Kharkov, Usp. Sovrem. Radioelektron., 3, 55-70.

Ancapichún, S. and J. Garcés-Vargas (2015). Variability of the Southeast Pacific Subtropical Anticyclone and its impact on sea surface temperature off north-central Chile, Cienc. Mar., 41, 1-20.

Anderson, J. (1999). Meteorological changes during a solar eclipse, Weather, 74, 207-215.

Anderson, R.C. and D.R. Keefer (1975). Observation of the temperature and pressure changes during the 30 June 1973 solar eclipse, J. Atmos. Sci., 32, 228-231.

Anderson, R.C., D.R. Keefer and O.E. Myers (1970). Atmospheric pressure and temperature changes during the 7 March, 1970 solar eclipse, J. 205 Atmos. Sci., 29, 583-587.

Antonia, R.A., A.J. Chambers, D. Phong-Anant, S. Rajagopalan and K.R. Screenivasan (1979). Response of atmospheric surface layer turbulence to a partial solar eclipse, J. Geophys. Res., 84, 1689-1692.

Aplin, K.L. and R.G. Harrison (2003). Meteorological effects of the eclipse of 11th August 1999 in cloudy and clear conditions, Proc. R. Soc. Lond. A, 459, 353-371.

Aplin, K.L., C.J. Scott and S.L. Gray (2016). Atmospheric changes from solar eclipses, Phil. Trans. R. Soc. A, 374, 20150217.

Association of Universities for Research in Astronomy (2019). AURA - Chilean Eclipse 2019, https://www.eclipse-solar.cl/

Avaria, S., J. Carrasco, J. Rutllant and E. Yañez (2004). El Niño-La Niña 1997-2000: their effects on Chile, Comité Oceanográfico Nacional-CONA, Valparaíso, Chile [in Spanish].

Bencze, P., B. Heilig, B. Zieger, J. Szendrói, J. Verö, H. Lühr, K. Yumoto, Y. Tanaka and J. Střeštík (2007). Effect of the August 11, 1999 total solar eclipse on geomagnetic pulsations, Acta Geod. Geoph. Hung., 42, 23-58.

Bischoff-Gauß, I., N. Kalthoff, S. Khodayar, M. Fiebig-Wittmaack and S. Montecinos (2008), Model simulations of the boundary-layer evolution over an arid Andes valley, Bound.-Layer Meteorol., 128, 357-379.

Blumthaler, M., A. Bais, A. Webb, S. Kazadzis, R. Kift, N. Kouremeti, B. Schallhart and A. Kazantzidis (2006). Variations of solar radiation at the Earth's surface during the total solar eclipse of 29 March 2006, in: Proc. SPIE 6362, Remote Sensing of Clouds and the Atmosphere, XI, 63620F.

Bojkov, R. (1968). The ozone variations during the solar eclipse of 20 May, 1966, Tellus, 20, 417-421.

Calamas, D.M., C. Nutter and D.N. Guajardo (2019). Effect of 21 August 2017 solar eclipse on surface-level irradiance and ambient temperature, Int. J. Energy Environ. Eng., 10, 147-156.

Chakrabarty, D.K., N.C. Shah and K.V. Pandya (1997). Fluctuations in ozone column over Ahmenabad during the solar eclipse of 24 October, 1995, Geophys. Res. Lett., 24, 3001-3003.

Chudzyński, W., A. Czyżewski, K. Ernst, A. Pietruczuk, W. Skubiszak, T. Stacewicz, K. Stelmaszczyk, A. Szymański, I. Sówka, A. Zwoździak and J. Zwoździak (2001). Observation of ozone concentration during the solar eclipse, Atmos. Res., 57, 43-49.

Chung, Y.S., H.S. Kim and S.H. Choo (2010). The solar eclipse and associated atmospheric variations observed in South Korea on 22 July 2009, Air Qual. Atmos. Health, 3, 125-130.

Clayton, H.H. (1901). Clayton's eclipse cyclone and the diurnal ciclones, Science 13, 747-750.

Curto, J.J., B. Heilig and M. Piñol (2006). Modeling the geomagnetic effects caused by the solar eclipse of 11 August 1999, J. Geophys. Res., 11, A07312.

Economou, G., E.D. Christou, A. Giannakourou, E. Gerasopoulos, D. Georgopoulo, V. Kotoulas, D. Lyra, N. Tsakalis, M. Tziortzou, P. Vahamidis, E. Papathanassiou and A. Karamanos (2008). Eclipse effects on field crops and marine zooplankton: the 29 March, 2006 total solar eclipse, Atmos. Chem. Phys., 8, 4665-4676.

Falvey, M. and R.D. Garreaud (2009). Regional cooling in a warming world: recent temperature trends in the southeast Pacific and along the west coast of subtropical South America (1979-2006), J. Geophys. Res., 114, D04102.

Fernández, W., V. Castro and H. Hidalgo (1993). Air temperature and wind changes in Costa Rica during the total solar eclipse of July 11, 1991, Earth Moon Planets, 63, 133-147.

Fernández, W., H. Hidalgo, G. Coronel and E. Morales (1996). Changes in meteorological variables in Coronel Oviedo, Paraguay, during the total solar eclipse of 3 November 1994, Earth Moon Planets, 74, 49-59.

Fiebig-Wittmaack, M., O. Astudillo, E. Wheaton, V. Wittrock, C. Perez and A. Ibacache (2012). Climatic trends and impact of climate change on agriculture in an arid Andean valley, Clim. Change, 111, 819-833.

Founda, D., D. Melas, S. Lykoudis, I. Lisaridis, E. Gerasopoulos, G. Kouvarakis, M. Petrakis and C. Zerefos (2007). The effect of the total solar eclipse of 29 March 2006 on meteorological variables in Greece, Atmos. Chem. Phys., 7, 5543-5553.

Geiger, R. (1954). Klassifikation der Klimate nach W. Köppen [Classification of climates afterW. Köppen], Landolt-Börnstein – Zahlenwerte und Funktionen aus Physik, Chemie, Astronomie, Geophysik und Technik, alte Serie, Springer, Berlin, Germany [in Germany].

Geiger, R. (1961). Überarbeitete Neuausgabe von Geiger, R.: Köppen-Geiger / Klima der Erde, Klett-Perthes Verlag, Gotha, Germany [in Germany].

Gerasopoulos, E., C.S. Zerefos, I. Tsagouri, D. Founda, V. Amiridis, A.F. Bais, A. Belehaki, N. Christou, G. Economou, M. Kanakidou, A. Karamanos, M. Petrakis and P. Zanis (2008). The Total Solar Eclipse of March 2006: overview, Atmos. Chem. Phys., 8, 5205-5220.

Gray, S.L. and R.G. Harrison (2012). Diagnosing eclipse-induced wind changes, Proc. R. Soc. A, 468, 1839-1850.

Hanna, E. (2000). Meteorological effects of the solar eclipse of 11 August 1999, Weather, 55, 430-446.

Hanna, E., J. Penman, T. Jónsson, G.R. Bigg, H. Björnsson, S. Sjúrdarson, M.A. Hansen, J.C. Cappelen and R.G. Bryant (2016), Meteorological effects of the solar eclipse of 20 March 2015: analysis of UK Met Office automatic weather station data and comparison with automatic weather station data from the Faroes and Iceland, Phil. Trans. R. Soc. A, 374, 20150212.

Harrison, G. and S. Gray (2017). The weather's response to a solar eclipse, Astron. Geophys., 58, 4.11-4.16.

Hassan, A.H. and U.A. Rahoma (2010). Solar Radiation at Total Solar Eclipse, 29 March 2006, at Tobruq, Am. J. Environ. Sci., 6, 449-454.

Ilić, L., M. Kuzmanoski, P. Kolarž, A. Nina, V. Srećković, Z. Mijić, J. Bajčetić and M. Andrić (2018). Changes of atmospheric properties over Belgrade, observed using remote sensing and in situ methods during the partial solar eclipse of 20 March 2015, J. Atmos. Sol.-Terr. Phys., 171, 250-259.

Juliá, C., D.A. Rahn and J.A. Rutllant (2012). Assessing the influence of the MJO on strong precipitation events in subtropical, semi-arid northcentral Chile (30°S), J. Clim., 25, 7003-7013.

Kalthoff, N., I. Bischoff-Gauß, M. Fiebig-Wittmaack, F. Fiedler, J. Thürauf, E. Novoa, C. Pizarro, R. Castillo, L. Gallardo, R. Rondanelli and M. Kohler (2002). Mesoscale wind regimes in Chile at 30°S, J. Appl. Meteorol., 41, 953-970.

Klein, M. and N. Robinson (1952). Solar Eclipse of 25 February 1952 and its Influence on the Insolation and on Various Meteorological Element, Israel Meteor. Ser. Meteor., Notes No. 11.

Kolarž, P., J. Šekarić, B.P. Marinković and D.M. Filipović (2005). Correlation between some of the meteorological parameters measured during the partial solar eclipse, 11 August, 1999, J. Atmos. Sol.-Terr. Phys., 67, 1357-1364.

Krishnan, P., P.K. Kunhikrishnan, S. Muraleedharan Nair, S. Ravindran, R. Ramachandran, D. B. Subrahamanyam and M. Venkata Ramana (2004). Observations of the atmospheric surface layer parameters over a semi arid region during the solar eclipse of August 11th, 1999, J. Earth Syst. Sci., 113, 353-363.

Lazzús, J.A. and I. Salfate (2017). Long-term prediction of wind speed in La Serena city (Chile) using hybrid neural network-particle swarm algorithm, Earth Sci. Res. J., 21, 29-35.

Littmann, M., K. Willcox and F. Espenak (2008). Totality - Eclipses of the Sun, Oxford University Press, 3rd ed.

Mantua, N.J., S.R. Hare, Y. Zhang, J.M. Wallace and R.C. Francis (1997). A Pacific Interdecadal Climate Oscillation with impacts on salmon production, Bull. Am. Meteorol. Soc., 78, 1069-1079.

Maturilli, M. and C. Ritter (2016). Surface radiation during the total solar eclipse over Ny-Ålesund, Svalbard, on 20 March 2015, Earth Syst. Sci. Data, 8, 159-164.

Namboodiri, K.V.S., P.K. Dileep, K. Mammen, G. Ramkumar, N.V.P. Kiran Kumar, S. Sreenivasan and R.K. Manchanda (2011). Effects of annular solar eclipse of 15 January 2010 on meteorological parameters in the 0 to 65 km region over Thumba, India, Meteorol. Z., 20, 635-647.

National Oceanic and Atmospheric Administration (2017). Earth System Research Laboratory, Physical Sciences Division, Boulder, CO, USA, http://www.esrl.noaa.gov/psd/.

Nishanth, T., N. Ojha, M.K. Satheesh Kumar and M. Naja (2011). Influence of solar eclipse of 15 January 2010 on surface ozone, Atmos. Environ., 45, 1752-1758.

Nymphas, E.F., M.O. Adeniyi, M.A. Ayoola and E.O. Oladiran (2009). Micrometeorological measurements in Nigeria during the total solar eclipse of 29 March, 2006, J. Atmos. Sol.-Terr. Phys., 71, 1245-1253.

Nymphas, E.F., T.A. Otunla, M.O. Adeniyi and E.O. Oladiran (2012). Impact of the total solar eclipse of 29 March 2006 on the surface energy fluxes at Ibadan, Nigeria, J. Atmos. Sol.-Terr. Phys., 80, 28-36.

Obrecht, A. (1893). El eclipse de sol del 16 de abril: su observación en Chile, Anales de la Universidad de Chile, 84, 260-264 [In Spanish].

Ojobo, E., D. Okoh, D. Okeya, N. Yusuf and G. Adukwu (2017). The Response of Meteorological Parameters to the September 1 2016 Solar Eclipse as Observed in Anyigba, Nigeria, Research and Reviews: J. Space Sci. Techn., 6, 16-24.

Peñaloza Murillo, M.A. and J.M. Pasachoff (2018). Cloudiness and solar radiation during the longest total solar eclipse of the 21st century at Tianhuangping (Zhejiang), China, J. Geophys. Res., 123, 13 443-13 461.

Pleijel, H. (2008). Observations of temperature and air humidity during the total solar eclipse 29 March 2006 at Side, Turkey, Meteorol. Z., 18, 107-109.

Power, S., T. Casey, C. Folland, A. Colman and V. Mehta (1999). Interdecadal modulation of the impact of ENSO on Australia, Clim. Dyn., 15, 319-324.

Prenosil, T. (2000). The influence of the 11 August 1999 total solar eclipse on the weather over central Europe, Meteorol. Z., 9, 351-359.

Reda, I. (2015). Solar eclipse monitoring for solar energy applications, Solar Energy, 112, 339-350.

Rosenbluth, B., H. Fuenzalida and P. Aceituno (1997). Recent temperature variations in Southern South America, Int. J. Climatol., 17, 67-85.

Salfate, I., C.H. López-Caraballo, C. Sabín-Sanjulián, J.A. Lazzús, P. Vega, F. Cuturrufo and J. Marín (2018). 24-hours wind speed forecasting and wind power generation in La Serena (Chile), Wind Eng., 42, 607-623.

Schulz, A., C. Schaller, M. Maturilli, J. Boike, C. Ritter and T. Foken (2017). Surface energy fluxes during the total solar eclipse over NyÅlesund, Svalbard, on 20 March 2015, Meteorol. Z., 26, 431-440.

Schulz, N., J.P. Boisier and P. Aceituno (2011). Climate change along the arid coast of northern Chile, Int. J. Climatol., 32, 1803-1814.

Stankov, S.M., N. Bergeot, D. Berghmans, D. Bolsée, C. Bruyninx, J.-M. Chevalier, F. Clette, H. DeBacker, J. DeKeyser, E. D'Huys, M. Dominique, J.F. Lemaire, J. Magdalenić, C. Marqué, N. Pereira, V. Pierrard, D. Sapundjiev, D.B. Seaton, K. Stegen, R. van der Linden, T.G.W. Verhulst and M.J. West (2017). Multi-instrument observations of the solar eclipse on 20 March 2015 and its effects on the ionosphere over Belgium and Europe, J. Space Weather Space Clim., 7, A19.

Szalowski, K. (2002). The effect of the solar eclipse on the air temperature near the ground, J. Atmos. Sol.-Terr. Phys., 64, 1589-1600.

Tzanis, C., C. Varotsos and L. Viras (2008). Impacts of the solar eclipse of 29 March 2006 on the surface ozone concentration, the solar ultraviolet radiation and the meteorological parameters at Athens, Greece, Atmos. Chem. Phys., 8, 425-430.

Veit, H. (1993). Quaternary landscape and climate evolution in the Norte Chico (northern Chile): an overview, Mt. Res. Dev., 13, 139-144.

Vogel, B., M. Baldauf and F. Fiedler (2001). The influence of a solar eclipse on temperature and wind in the Upper-Rhine Valley – A numerical case study, Meteorol. Z., 10, 207-214.

Winkler, P., U. Kaminski, U. Köhler, J. Reidl, H. Schroers and D. Anwender (2001). Development of meteorological parameters and total ozone during the total solar eclipse of Agust 11, 1999, Meteorol. Z., 10, 193-199.

Zerefos, C.S., D.S. Balis, C. Meleti, A.F. Bais, K. Tourpali, K. Vanicek, F. Cappenlanni, U. Kaminski, T. Colombo, R. Stubi, P. Formenti and M.O. Andreae (2000). Changes in surface solar UV irradiances and total ozone during the solar eclipse of August 11, 1999, J. Geophys. Res., 105, 26 463-26 473.

Zerefos, C.S., D.S. Balis, P. Zanis, C. Meleti, A.F. Bais, K. Tourpali, D. Melas, I. Ziomas, E. Galani, K. Kourtidis, A. Papayannis and Z. Gogosheva (2001). Changes in surface UV solar irradiance and ozone over the Balkans during the eclipse of 11 August 1999, Adv. Space Res., 27, 1955-1963.

*CORRESPONDING AUTOR: Juan A. LAZZÚS,
Departamento de Física, Universidad de La Serena, Casilla 554, La Serena, Chile and
Instituto de Investigación Multidisciplinario en Ciencias y Tecnología, Universidad de La Serena, Casilla 554, La Serena, Chile,
email: jlazzus@userena.cl